Journal of Thermal Analysis, Vol. 52 (1998) 595-607

SYNTHESIS OF ULTRAFINE COBALT FERRITE BY THERMAL DECOMPOSITION OF CITRATE PRECURSOR

*S. Prasad, A. Vijayalakshmi and N. S. Gajbhiye**

Departmant of Chemistry. Indian Institute of Technology, Kanpur 208016, U. P. India

(Received September 27, 1997)

Abstract

Ultrafine particle of $CoFe_2O_4$ has been synthesized using citrate precursor technique. Thermal decomposition of the citrate precursor, $Co_3Fe_6O_4(C_6H_6O_7)_8 \cdot 6H_2O$, was investigated by TG, DTA and DTG techniques, gas and chemical analyses and was found to decompose in one or two major steps depending on the heating rate in static/flowing air atmosphere. In the lower heating rate (5°C min^{-1}), metastable acetonedicarboxylate complex was isolated with the evolution of CO gas and coordinated water molecule in the temperature range of 120–220°C. Complete decomposition of the citrate network occurs between 220–330°C with the simultaneous evolution of CO_2 and acetone. However both these steps appeared as simultaneous and/or single step process (between 120–160°C), when the heating rate is high (10°C min^{-1} and above). The ultrafine $CoFe_2O_4$ particles are observed as the aggregates having surface area 133.8 $m^2 g^{-1}$ composed of 4.8 nm crystallites. The citrate precursor and the decomposed products were characterized by IR, NMR, XRD, SEM and surface area measurements.

Keywords: citrate, precursor, thermal decomposition, ultrafine

Introduction

Preparation of ultrafine particles of ferrites has been the subject of extensive study because of their wide range of applications and their importance in understanding the theories of magnetism. The preparation of spinel ferrites has been for long time technologically important to the microwave industries. In the past decade or so the production of ferrites with small particles has been important for high speed digital tapes or disc recording [1]. It has the future application as a repulsive suspension for use in levitated railway systems [2]. This has prompted several investigators to synthesize the ultrafine ferrite particles [3–5]. Synthesis of ultrafine cobalt ferrite by citrate precursor technique is a continuation of our

* Author to whom all correspondence should be addressed.

1418–2874/98/ $ 5.00

Akadémiai Kiadó, Budapest
Kluwer Academic Publishers, Dordrecht

work on other spinel ferrites, hexaferrites and rare earth garnets [6–9]. No systematic efforts have been made on the synthesis of nanosized cobalt ferrite by citrate precursor technique and the studies do not report the thermal decomposition of cobalt iron citrate precursor. The present study describes our attempts to investigate the mode of decomposition of cobalt iron citrate precursor at varying heating rates which in turn governs the synthesis and characterization of amorphous and crystalline $CoFe_2O_4$.

Materials and methods

Preparation of cobalt iron citrate precursor

$Co_3Fe_6O_4(C_6H_6O_7)_8 \cdot 6H_2O$

90 ml, 0.1 M cobalt nitrate and 200 ml, 0.1 M citric acid (AnalaR grade from S.d. Fine-Chem Boisar India), were mixed with 0.1 M, 125 ml $Fe(NO_3)_3$ (GR grade from Loba Chemie Bombay, India) in the molar ratio of Co:Fe:Citric acid =1:2:2.7. The resultant homogeneous solution was refluxed for 20 h at 80°C in a 1 L capacity round bottomed flask. The refluxed solution was slowly evaporated on a water bath to form a viscous liquid which was later transferred to a petridish. Further drying was carried out at 120°C in an oven for 5 h to remove adsorbed water. During the process of drying the gel swells into a fluffy mass which eventually breaks into the brittle flakes. The cobalt iron citrate precursor was found to be hygroscopic in nature and the degree of hydration varied from 2 to 8 per mol.

Analysis of citrate precursor

Fe was estimated gravimetrically with 5% cupferron and subsequently weighed as Fe (III) oxide [10]. Iron was also analysed volumetrically after reducing Fe^{3+} to Fe^{2+} by $SnCl_2$. 10 ml saturated solution of $HgCl_2$ was added at one stroke. The resultant curdy white precipitate ensures that excess of $SnCl_2$ is not present. To this properly reduced solution 10 ml of 30% phosphoric acid solution and a few drops of sodium diphenylamine sulphonate indicator was added and titrated with $K_2Cr_2O_7$ solution to change the colour of the solution from green to gray green till the appearance of the purple or violet blue colour [11]. Cobalt and Fe were also analysed by using Atomic Absorption Spectroscopy model AA-10 Varian, U.S.A., to ensure the stoichiometry. The results from both the analyses agreed very well for the precursor, intermediates and the end product. Citrate contents in the precursor was estimated using Karpov's method in which 2 ml of citrate precursor solution was mixed with 25 ml of 0.1 N $K_2Cr_2O_7$ and 5 ml conc. H_2SO_4. The solution was heated gently and the excess of dichromate was titrated *vs.* 0.1 N solution of Mohr's salt using 3 to 4 drops of 0.1% Phenylanthranilic acid as an indicator. The end point is the change of red violet to green colour [12]. The presence of acetone was also detected by Iodoform test and 2,4 diphenyl hy-

drazone test. The evolution of acetone during thermal decomposition was further confirmed by ^{1}H NMR spectral analysis using JEOL-PMX-6031 [13]. Quantitative analysis of acetone was done by titrating excess of acidified 0.1 N Iodine solution *vs.* 0.1 N $Na_2S_2O_3$ solution in the presence of 1 N NaOH.

Experimental techniques

Thermal analysis of the cobalt iron citrate precursor were carried out by using simultaneous TG and DTA upto 700°C with a Linseis, L-81/042 derivatograph. Samples of 60 mg were placed in a platinum crucible, ignited alumina was used as the reference material with the heating rate of 5 and 10°C min^{-1}. The thermal analyses were carried out in a static/flowing air atmosphere at the rate of 60 ml min^{-1}. Some TG were also recorded on DuPont 2100. Perkin Elmer 240 elemental analyser was used to analyse the evolved gases. IR spectra were recorded with a Perkin Elmer 377, spectrometer using sample in the form of KBr pellets. ^{1}H NMR spectra was recorded using JEOL-PMX-6031 Japan. X-ray diffractograms were recorded using a Rich Seifert Isodebyflex, X-ray unit 2002 with CuK_α radiation and Ni filter. Surface area measurement was done using the single point BET method with Micrometrics Pulse Chemisorb 2700 using nitrogen gas as the adsorber. Degassing is done by heating the sample at 200°C and flushing He gas. The particle size and the morphology of the samples were studied using SEM, JEOL-JSM-840 A.

Results

After chemical analysis of anhydrous cobalt iron citrate precursor, the amount of Co=7.9%, Fe=15.8%, H_2O=4.8%, citrate=69.0% corroborated the stoichiometry; $Co_3Fe_6O_4(C_6H_6O_7)_8{\cdot}6H_2O$. The precursor was amorphous to X-rays. The IR spectra of cobalt iron citrate precursor, citric acid and $Fe(NO_3)_3$ were analysed and are summarized in Table 1. The IR bands for citrate precursor were found to be broad in nature having all the common bands of citric acid. The broad bands in the region 3600–3000 cm^{-1} and around 1610 cm^{-1} can be due to the stretching and bending modes of water molecules because the intensity of these absorption decreases and disappears with the heat treatment temperature. However the broad band in the region 3429 cm^{-1} and the small shoulder at 1700 cm^{-1} could be attributed to the free hydroxyl and carboxylate group of cobalt iron citrate. The broad and the unresolved bands at 1570, 1400 cm^{-1} are characteristic of completely ionised carboxyl group with equalised CO bands. No bands were observed for free citric acid (1700 cm^{-1}, *vs.*). On the basis of IR spectral analysis we have invoked that the citrate groups coordinates to the Fe and Co metal through carboxylate groups leaving free

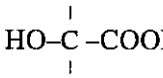

HO–C –COOH groups.

Table 1 IR spectral frequency assignments for citric acid, ferric nitrate, precursor and different heat treated products

Citric acid	$Fe(NO_3)_3$	Precursor	Heat treated temperature/°C				Assignments
			160	220	280	330	
3300s	3700–3000vs	3700–3000vs	3700–3000w	3700–3000w	–	–	νOH water
3450sh	–	3450sh	–	–	–	–	νOH hydroxyl
2900–2800s	–	2900–2800w	2900–2800w	–	–	–	νCH
–	–	–	–	–	2320w	2320w	νCO_2
1700vs	–	1700vwsh	–	–	–	–	νasym C=O
1620w	1610s	1610w	–	–	–	–	δHOH
–	–	1570vs	1570w	–	–	–	νasym COO
1430, 13951, 355s	–	1400vs	1400w	–	–	–	νsym COO
–	1361vs	–	–	–	–	–	$\nu_3 NO_3^-$
1240–1190s	–	–	–	–	–	–	νsym CO
1080–1055s	–	1270wsh	1080br	–	–	–	νst C–O
940–900sh	–	1080br	–	–	–	–	citrate
	835m	–	–	–	–	–	$\nu_2 NO_3^-$
780sh	–	–	–	–	–	–	citrate
600, 650sh	–	–	–	–	–	–	citrate
–	–	–	–	–	575w	575m	$\nu_1 CoFe_2O_4$
–	–	–	–	–	374w	374m	$\nu_2 CoFe_2O_4$

s – strong; vs – very strong; sh – sharp; m – medium; w – weak; br – broad

Thermal decomposition of citrate precursor

Thermal curves recorded in static/flowing air atmosphere at 5 and 10°C min^{-1} are shown in Figs 1 and 2. It can be seen that one to one correlation exists between TG, DTG and DTA curves indicating that the thermal effects are accompanied by mass loss. There are two major steps in the decomposition. The probable reactions are, decomposition of precursor to acetonedicarboxylate complex and its final decomposition to cobalt ferrite. DTA shows there is one endotherm and two exotherms. Endotherm corresponds to the removal of the adsorbed water whereas two exotherms corresponds to the citrate decomposition followed by the formation of crystalline $CoFe_2O_4$. Interestingly, the two steps

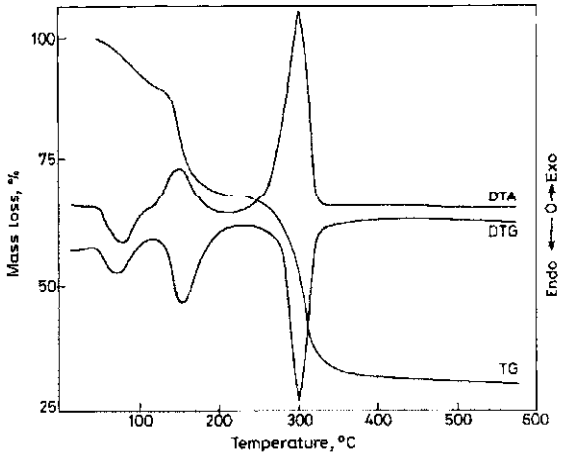

Fig. 1 TG, DTG and DTA recorded at 5°C min^{-1} of cobalt iron citrate precursor

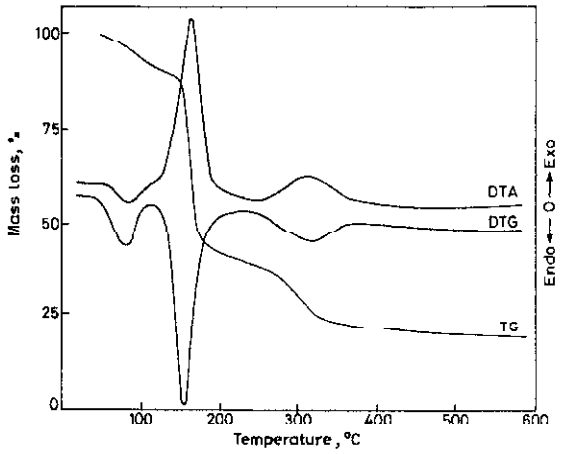

Fig. 2 TG, DTG and DTA recorded at 10°C min^{-1} of cobalt iron citrate precursor

were found to take place in single step when the heating rate was 10°C min^{-1}. These can be seen from an intense exotherm between 120–160°C and a broad exotherm between 220–330°C . Intense exotherm corresponds to the decomposition of citrate network with the simultaneous evolution of CO, CO_2, acetone and water vapour and the broad exotherm around 280°C corresponds to the crystallization of the amorphous phase, which is also evident from the XRD pattern. The complete data of the observed and the calculated mass loss with their corresponding temperature ranges are given in the Table 2.

Mode of decomposition of citrate precursor

i) Formation of acetonedicarboxylate complex

Depending on the heating rate, thermal decomposition of the cobalt iron citrate precursor was found to be the most important and at the same time most complex process. The citrate precursor is probably converted to metastable acetonedicarboxylate complex. This process was found to be exothermic in air atmosphere (Fig. 1) and spontaneously large amount of gases are evolved. The decomposition of the citrate precursor starts around 120°C with the simultaneous evolution of CO and H_2O. The mass loss of 16.8% was recorded upto 220°C as compared to the calculated value of 15.1% for the formation of acetonedicarboxylate complex $Co_3Fe_6O_4(C_5H_6O_6)_8$ (Table 2). Evolution of large amount of CO gas on combustion, i.e. secondary reaction of CO makes the process exothermic in air atmosphere [15]. Less intense exotherm is because of the simultaneous evolution of coordinated water. At the end of this step, on isothermal heating of the precursor, the metastable acetonedicarboxylate complex can be isolated which on analysis gave; Co=8.1%, Fe=16.2 %, acetonedicarboxylate=70.4% which were comparable with the calculated values; Co=9.4%, Fe=17.9% acetonedicarboxylate complex=72.7%

ii) Decomposition of acetonedicarboxylate complex

The acetonedicarboxylate complex started decomposing above 220°C and the decomposition was completed around 330°C . At this stage the observed mass loss was found to be 40.5% compared to the calculated 41.0%. Decomposition of the acetonedicarboxylate involves the decarboxylation process with the simultaneous evolution of acetone molecules formed.

The evolution of acetone was confirmed by heating the anhydrous cobalt iron citrate precursor in a closed hard glass tube and the evolved acetone was condensed in an ice cold $CDCl_3$. The NMR spectrum show the acetone proton peak at δ=2.2 ppm, thus indicating the evolution of acetone molecules formed. That means when the precursor is decomposed at higher temperature above 280°C, the citrate network collapses with the formation of $CoFe_2O_4$. The residue at this stage has a structure corresponding to $CoFe_2O_4$ with trapped CO_2 gas; $3(CoFe_2O_4)\cdot 6CO_2$ because of its fine particle nature and large surface area. It is

Table 2 Mass loss in decomposition steps of $Cs_3Fe_6O_4(C_6H_6O_7)_8 \cdot 6H_2O$ recorded with varying heating rate

Steps	Temperature range/°C	Heating rate/5°C min^{-1}		Steps	Temperature range/°C	Heating rate/10°C min^{-1}	
		obs. wt. loss/ %	cal. wt. loss/ %			obs. wt. loss/ %	cal. wt. loss/ %
1	<120	9.7	–	1	<120	9.3	–
2	120–220	16.8	15.1	2	120–160	41.8	40.1
3	220–330	40.5	41.0	3	160–330	28.4	27.9
4	>330	12.6	11.9				

surprising that the decomposition does not go through the formation of complex carbonates as was reported in the literature [7, 8, 15–17]. This residue dissolves in conc. HCl and the black particles of carbon were not observed in the solution. The chemical analysis of the residue, $3[CoFe_2O_4 \cdot 2CO_2]$, shows the observed values, Co=16.2%, Fe=32.5% compared to the theoretical values, Co=18.3%, Fe=34.6%.

However, the decomposition process was found to be faster with the heating rate of 10°C min^{-1} (Fig. 2). This shows the precursor is a single step exothermic process leading to the formation of amorphous $3(CoFe_2O_4) \cdot 14CO_2$ with the simultaneous evolution of CO, CO_2 and acetone. The decomposition temperature range is 120–160°C . The observed mass loss of 41.8% agrees well with calculated value of 40.1% for the formation of amorphous cobalt ferrite with trapped CO_2 molecule. The adsorption of CO_2 gas is much larger in residue $3(CoFe_2O_4) \cdot 14CO_2$ because of its fine particle nature having high porosity and very large surface area. Isothermal heating of the citrate precursor around 280°C and above for 48 h yields a residue of the constant composition $CoFe_2O_4$ with the total mass loss of 69.9% compared with the 68.06% calculated for the above calculations (Table 2).

X-ray diffraction and IR spectral studies of the citrate precursor decomposition

Figure 3 shows the XRD patterns for the formation of intermediates and the spinel phase at various temperatures, when the precursor was heated at the rate of 10°C min^{-1}. The formation of pure single phase $CoFe_2O_4$ occurs around 200°C. Below 280°C $CoFe_2O_4$ phase is X-ray amorphous and it crystallises completely above this temperature. The assignments of the IR bands is shown in the

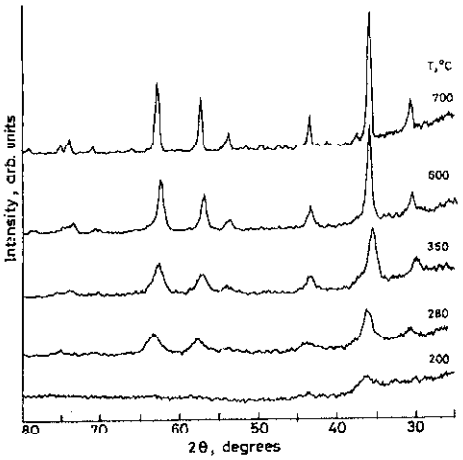

Fig. 3 X-ray diffraction patterns of decomposed products at various temperature

Table 1 for the intermediates and pure spinel phase. The absorption for citrate precursor occurs at 3429 (br), 2900 (w), 1700 (sh), 1570 (vs), 1400 (vs), 1270 (w) and 1080 (w) cm^{-1}. The 1700 (sh) and 1080 (w) cm^{-1} absorption band disappears above 160°C retaining carboxylate absorption at *1570* and *1400* cm^{-1} *[18]* which disappears above 220°C on heat treatment for 5h. The IR spectrum at 280°C and above shows bands at 575 cm^{-1} and 374 cm^{-1} which corresponds to the spinel phase formation and a sharp band at 2320 cm^{-1}, may be due to the assymetric stretching mode of free CO_2. The sharp absorption at 575 and 374 cm^{-1} is due to the lattice absorption of two CoO_4 and one FeO_4 group of tetrahedral symmetry in $CoFe_2O_4$ [19]. The increase in the intensity of these bands with heat treatment temperature above 320°C is understood in terms of the manifestation of the crystalline $CoFe_2O_4$.

Characterization of ultrafine $CoFe_2O_4$ particles

The final details of ultrafine $CoFe_2O_4$ particles and crystallites are presented in the electron micrograph in Fig. 4. The micrographs show that the amorphous $CoFe_2O_4$ consists of spherical particles having the size 34.1 nm (Fig. 4a). After the crystallization the particles are smaller in size with 22.7 nm and shows the

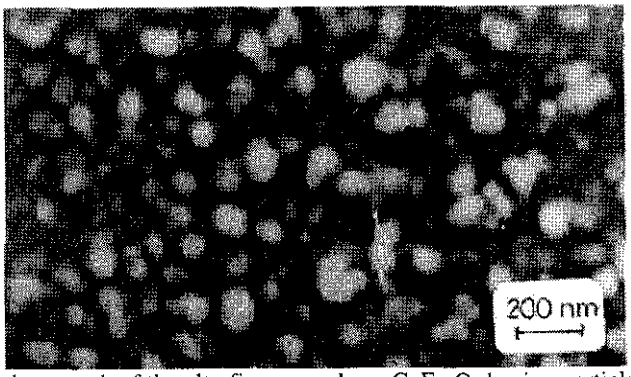

Fig. 4a SEM photograph of the ultrafine amorphous $CoFe_2O_4$ having particle size 34.1 nm

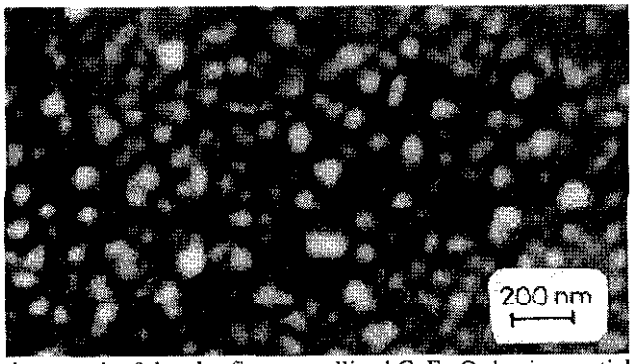

Fig. 4b SEM photograph of the ultrafine crystallized $CoFe_2O_4$ having particle size 22.7 nm

uniform distribution (Fig. 4b). The micrographs indicates the assembly of crystallites (aggregates) resulting larger particle size.

The BET surface areas were measured for the crystallized $CoFe_2O_4$ and for the amorphous $3(CoFe_2O_4)\cdot 14CO_2$ after degassing in order to remove the adsorbed CO_2. The surface area was found to be 74.8 $m^2\ g^{-1}$, 133.8 $m^2\ g^{-1}$ and corresponds to particle size 15.2 nm, 8.50 nm respectively. The reduction in the BET surface area is observed after crystallization above 280°C. The decrease in the surface area is due to the localised growth of the crystallites.

The particle size calculated from the SEM and BET surface area are relatively larger than the XRD crystallite size of 4.0 and 7.5 nm. These studies confirms the existence of an aggregate consisting of crystallites due to their high energetic surfaces which is a nonporous particle.

Discussion

Detailed studies are not available on citrate complexes for ferrite formation, however thermal decomposition studies of citrate complexes for the formation of garnets [20, 21], $LaCrO_3$ [22], $LaFeO_3$ [14], $LaCoO_3$, $LaCrO_3$, $SrCoO_3$ [23], $BaTiO_3$ [16] has been reported. In general these studies shows that an impure citrate metal complex decomposition involve mainly three to four steps, which are as follows; removal of water of hydration and excess nitrate, decomposition of anhydrous citrate complex and free citric acid through the intermediates like aconitate, itaconate, itaconic anhydride and complex carbonates leading to the respective oxides. In most of these cases citric acid and nitrates were present in considerable proportion [14, 24] thus the thermal decomposition studies are not comprehensive and remain inconclusive.

We have studied successfully and reported the thermal decomposition of hexahydrated nickel iron citrate [6] and strontium iron citrate precursor [7]. In the present studies neither free citric acid nor nitrates were present in the precursor. To predict the number of citric acid molecules associated with the metallic ions, the knowledge of citrate precursor structure is very useful. However little evidence is available in the literature concerning the possible structural arrangements of cobalt iron citrate complex, though the citrate complex of cobalt and iron have been reported independently [25, 26]. The extent of polymerization in the citrate complexes depends on pH [27, 28] and in the lower pH ranges the extent of polymerization is not sufficient to form the network of solid structures, therefore the cobalt iron citrate precursor is obtained in the pH range of 1.0–2.0. Also it was difficult to predict the metal ion sites binding with the citric acid; therefore on the basis of thermal analyses, chemical analyses and gas analyses, XRD, IR and NMR data a plausible mechanism has been proposed. Cobalt iron citrate precursor decomposes to $CoFe_2O_4$ phase in air atmosphere and the experimental results indicate the following scheme:

For heating rate: 5°C min^{-1}

1. $Co_3Fe_6O_4(C_6H_6O_7)_8 \cdot (n+6)H_2O \xrightarrow[<120°C]{} Co_3Fe_6O_4(C_6H_6O_7)_8 \cdot 6H_2O + nH_2O$

2. $Co_3Fe_6O_4(C_6H_6O_7)_8 \cdot 6H_2O \xrightarrow[120–220°C]{} Co_3Fe_6O_4(C_5H_6O_6)_8 + 6H_2O + 8CO$

3. $Co_3Fe_6O_4(C_5H_6O_6)_8 \xrightarrow[220–330°C]{} 3CoFe_2O_4 \cdot 6CO_2 + 10CO_2 + 8CH_3COCH_3$

4. $Co_3Fe_6O_{12}(CO_2)_6 \xrightarrow[>330°C]{} 3CoFe_2O_4 + 6CO_2$

For heating rate: 10°C min^{-1}

1. $Co_3Fe_6O_4(C_6H_6O_7)_8 \cdot (n+6)H_2O \xrightarrow[<120°C]{} Co_3Fe_6O_4(C_6H_6O_7)_8 \cdot 6H_2O + nH_2O$

3. $Co_3Fe_6O_4(C_6H_6O_7)_8 \xrightarrow[120–160°C]{} 3CoFe_2O_4 \cdot 14CO_2 + 8CO + 8H_2O + 2CO_2 + 8(CH_3COCH_3)$

4. $Co_3Fe_6O_{12}(CO_2)_{14} \xrightarrow[160–330°C]{} 3CoFe_2O_4 + 14CO_2$

Hexahydrated cobalt iron citrate precursor was isolated by removing extra water adsorbed around 120°C. The first step represents the major reaction in the thermal decomposition of the cobalt iron citrate precursor. During this process removal of coordinated water and CO gas results in the formation of metastable acetonedicarboxylate complex, $Co_3Fe_6O_4(C_5H_6O_6)_8$. In the second step the complete internal conversion of carboxylate groups, methylene and hydroxyl groups takes place to form acetone and CO_2 gas which can be observed by the disappearance of 2900 cm^{-1} ($\nu_{sym.}CH$), 1570 cm^{-1}($\nu_{asym.}COO$), 1400 cm^{-1} ($\nu_{sym.}COO$) absorption bands in the IR spectrum. Gases evolved mainly CO and acetone were confirmed by the gas analysis data. Some amounts of CO_2 gas is adsorbed in $CoFe_2O_4$ lattice because of the large surface area. It can be seen from the 2320 cm^{-1} absorption in the IR spectra of residue; However, when the heating rate is 10°C min^{-1} and above, steps 1 and 2 takes place simultaneously in one and/or single step at relatively much lower temperature (120–160°C). This occurs with the simultaneous evolution of large amount of gases (CO, CO_2, water vapour and acetone). The compound $3(CoFe_2O_4) \cdot 14\ CO_2$ was found to be X-ray amorphous and the adsorbed CO_2 gas disappears only by heating around 250°C for more than one day. The actual reaction for the formation of $CoFe_2O_4$ appears to be simpler in this step unlike the reaction proceeding through aconitate complex formation analogy with the thermal decomposition of barium titanyl citrate complex [16].

It is very interesting to note that the decomposition does not undergo through the formation of complex carbonates as reported earlier [7, 16] and pure phase forms unusually at much lower temperature i.e. 200°C . The complete crystallization of this amorphous phase takes place above 280°C which is confirmed by its XRD pattern (Fig. 3). High decomposition rate, low decomposition temperature and the simultaneous evolution of large amount of gases results in the formation of ultrafine amorphous and crystalline $CoFe_2O_4$ particles which shows the extraordinary magnetic behaviour in some fundamental ways. The crystalline phase of $CoFe_2O_4$ shows the crystallite size of about 7.5 nm from the X-ray line width measurement using the Scherer method [29]. The particle size calculated from the SEM and BET surface area are relatively larger than the XRD crystallite size. SEM and BET surface area measurement confirms the existence of an aggregate consisting of crystallites due to their high energetic surfaces.

Conclusions

Ultrafine particles of $CoFe_2O_4$ ferrites has been synthesized using citrate precursor method and the mechanism of the thermal decomposition was examined in detail. The cobalt iron citrate precursor is found to have the formula $Co_3Fe_6O_4(C_6H_6O_7)_8 \cdot 6H_2O$ and the decomposition in air atmosphere results the formation of pure and stoichiometric $CoFe_2O_4$ phase. For lower heating rate ($5^\circ C\ min^{-1}$) the decomposition was found to occur in two major steps;

1) formation of acetonedicarboxylate complex with the evolution of water vapour and CO gas and 2) decomposition of acetonedicarboxylate complex to $CoFe_2O_4$ with the simultaneous evolution of CO_2 gas and the acetone molecules. However these two steps were found to occur simultaneously for the heating rate of $10^\circ C\ min^{-1}$. The formation of amorphous $3(CoFe_2O_4) \cdot 14CO_2$ occurs at relatively much lower temperature i.e. 200°C having surface area of 133.8 $m^2\ g^{-1}$ and corresponds to 8.5 nm particle size. The particle size calculated from the SEM (34.1 nm) and BET surface area are relatively larger than the XRD crystallite size (4.8 nm) and confirms the formation of crystallite aggregates.

* * *

We acknowledge the financial assistance during this investigation by the Department of Science and Technology, New Delhi.

References

1 T. Pannaparyil, R. Marande, S. Komarneni and S. G. Sarkar, J. Appl. Phys., 64 (1988) 5641.
2 A. Goldman, In Electronic Ceramics, edited by L. Levenson (Marcel Dekker, New York), (1988) 170.
3 T. Y. Tseng and T. C. Lin, J. Mater. Sci. Lett., 8 (1989) 261.
4 S. Komarneni and F. Elizabeta, J. Am. Ceram. Soc., 71 (1988) C 26.
5 K. Haneda and A. H. Morrish, J. Appl. Phys., 63 (1988) 4258.

6 N. S. Gajbhiye and S. Prasad, Thermochim Acta, 285 (1996) 325.
7 N. S. Gajbhiye and A. Vijayalakshmi, J. Thermal Anal., In Press.
8 V. K. Sankaranarayanan and N. S. Gajbhiye, Thermochim Acta, 153 (1989) 337.
9 V. K. Sankaranarayanan and N. S. Gajbhiye, J. Am. Ceram. Soc., 73 (1990) 1301.
10 A. I. Vogel, Text Book of Quantitative Inorganic Analysis, ELBS, England, 1986, p. 678.
11 N. Howell Furman, (Ed.) Standard Methods of Chemical Analysis Ed. 6, Vol. 1, Princeton New York 1962.
12 O. N. Karpov, Tr. Vses Nauchn. Issled Inst. Khim. Reaktivov, 25 (1963) 334.
13 C. J. Pouchart (Ed.) The Aldrich Library of NMR spectra, Edition 11, Vol. 1, 4580.
14 H. M. Zhang, Y. Teraoka and N. Yamazoe, Chem. Lett., 4 (1987) 665.
15 H. S. Gopalakrishnamurthy, M. Subharao and T. R. Narayanan Kutty, J. Inorg. Nucl. Chem., 37 (1975) 891.
16 D. Hennings and W. Mayr, J. Solid State Chem., 26 (1978) 329.
17 N. S. Gajbhiye, U. Bhattacharya and V. S. Darshane, Thermochim. Acta, 264 (1995) 219.
18 R. Nakamoto, Infrared and Raman Spectra of Inorganic and Coordination Compounds, John Wiley, New York 1978.
19 R. D. Waldron, Phys. Rev., 99 (1955) 1727.
20 Ph. Courty, H. Ajot, Ch. Marcilly and B. Delmon, Powder Technology, 7 (1973) 21.
21 Th. J. A. Popma and A. M. Van Diepen, Mater. Res. Bull., 9 (1974) 111.
22 J. M. D. Tascon, S. Mendioroz and L. Gonzalez Tejuca, Z. Phys. Chem. (N. F.), 124 (1981) 109.
23 D. J. Anderton and F. R. Sale, Powder Metall., 22 (1979) 14.
24 B. Delmon and J. Ehretsmann (Eds.) Fine particles, Electrochemical Society, Princeton, N. J., 1974, p. 242.
25 V. V. Grigor'eva and S. M. Tsimbler, Zh. Neorg. Khim., 13 (1968) 498.
26 E. Belloni Milan, Crazz Chimital, 50 (1920) 159.
27 C. J. Brinker and G.W. Scherrer, J. Noncryst. Sol., 70 (1985) 301.
28 C. J. Brinker and G. W. Scherrer, in L. L. Hench and D. R. Ulrich (Eds.), Ultrastructure processing of ceramics, Glass and composites, John Wiley, New York, 1985, p.43.
29 B. D. Cullity, Elements of X-ray diffraction, Edition Wesley, U.S.A., 1978, p.284.